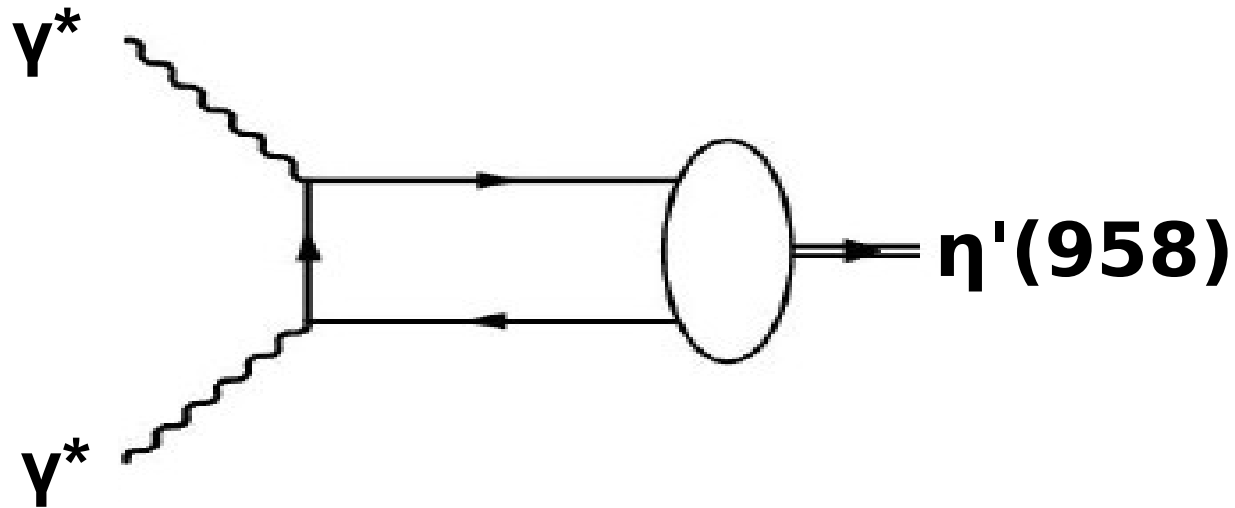


Study of $e^+e^- \rightarrow e^+e^-\eta'(958)$ in the double-tag mode at BABAR

Evgeny Kozyrev

Novosibirsk State University
Budker INP SB RAS, Novosibirsk, Russia

on behalf of the **BaBar collaboration**
Phys.Rev.D 98 (2018) 11, 112002



16th International Workshop on Meson Physics

online via ZOOM

17th - 20th May 2021

Outline

→ Introduction

Transition form factor (TFF) at large momentum transfers

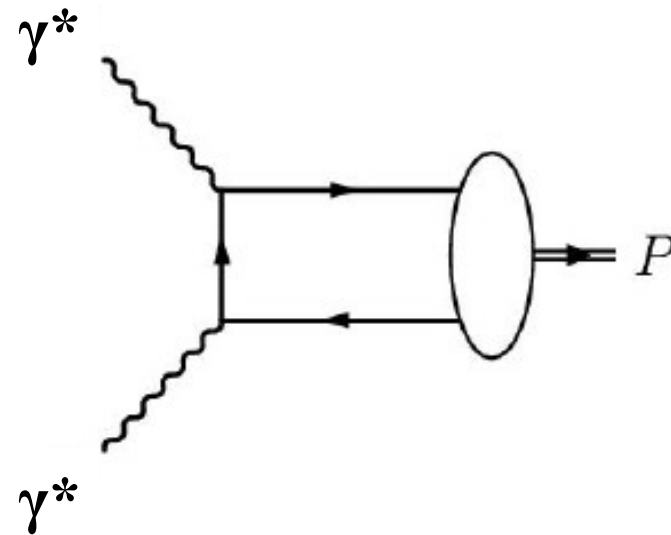
TFF at small momentum transfers

Existing experimental data

→ Measurement of the TFF of η' meson with BaBar detector

→ Comparison with theoretical predictions

→ Summary



The amplitude of the $\gamma^* \gamma^* \rightarrow P$ transition

$$A = e^2 \varepsilon_{\mu\nu\alpha\beta} e_1^\mu e_2^\nu q_1^\alpha q_2^\beta F(q_1^2, q_2^2),$$

P — pseudoscalar meson

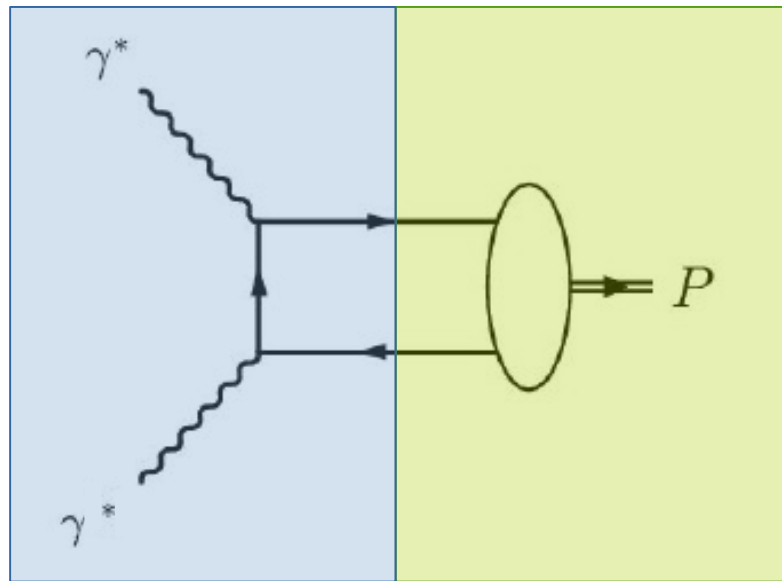
$e_{1,2}$ — photon polarization

$q_{1,2}$ — 4-momentum of photon

- there are a lot of experimental study of pseudoscalar meson production via the fusion of real (**on-shell**) and virtual (**off-shell**) photons $\gamma^* \gamma \rightarrow P$: π^0 , η , η' , η_c

- there are **no** measurements of the double **off-shell** transitions $\gamma^* \gamma^* \rightarrow P$

Introduction. $F(Q_1^2, Q_2^2)$ at **large** Q^2 .



Hard part

Warm part

$$F(Q_1^2, Q_2^2) = \int \mathbf{T}(x, Q_1^2, Q_2^2) \boldsymbol{\varphi}(x, Q_1^2, Q_2^2) dx$$

x - is the fraction of the meson momentum carried by one of the quarks

$\mathbf{T}(x, Q_1^2, Q_2^2)$ - hard scattering amplitude for $\gamma^* \gamma^* \rightarrow qq\bar{q}$ transition which is calculable in pQCD
 $\boldsymbol{\varphi}(x, Q_1^2, Q_2^2)$ - nonperturbative meson distribution amplitude (DA) describing transition $P \rightarrow qq\bar{q}$

$$T_H(x, Q_1^2, Q_2^2) = \frac{1}{2} \cdot \frac{1}{xQ_1^2 + (1-x)Q_2^2} \cdot \left(1 + C_F \frac{\alpha_S(Q^2)}{2\pi} \cdot t(x, Q_1^2, Q_2^2) \right) + (x \rightarrow 1-x) + O(\alpha_s^2) + O(\Lambda_{QCD}^4/Q^4)$$

NLO correction

[E. Braaten, Phys. Rev. D **28**, 3 (1983)]

- The meson DA $\boldsymbol{\varphi}(x, Q_1^2, Q_2^2)$ plays an important role in theoretical descriptions of many QCD processes. Its shape (x dependence) is unknown, however its universal asymptotic form:

At the limit $\mu \rightarrow \infty$ $\phi_P(x, \mu) = A_P 6x(1-x)(1 + O(\Lambda_{QCD}^2/\mu^2))$

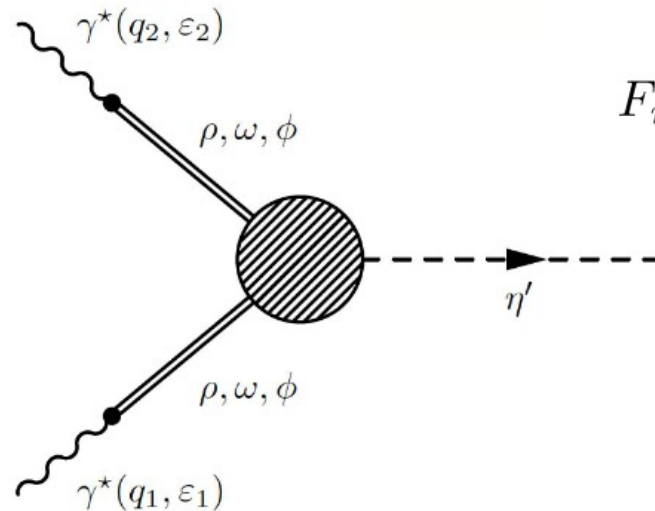
[S. J. Brodsky and G. P. Lepage, Phys. Rev. D **24**, 7 (1981)]

Introduction. $F(Q_1^2, Q_2^2)$ at low Q^2 .

- $F(0,0)$ is related to axial anomaly:

$$\Gamma_{\eta' \rightarrow 2\gamma} = \frac{\pi\alpha^2 m_{\eta'}^3}{4} |F(0,0)|^2 = 4.30 \pm 0.16 \text{ keV} \quad \rightarrow \quad F(0,0) = 0.342 \pm 0.006 \text{ GeV}^{-1}.$$

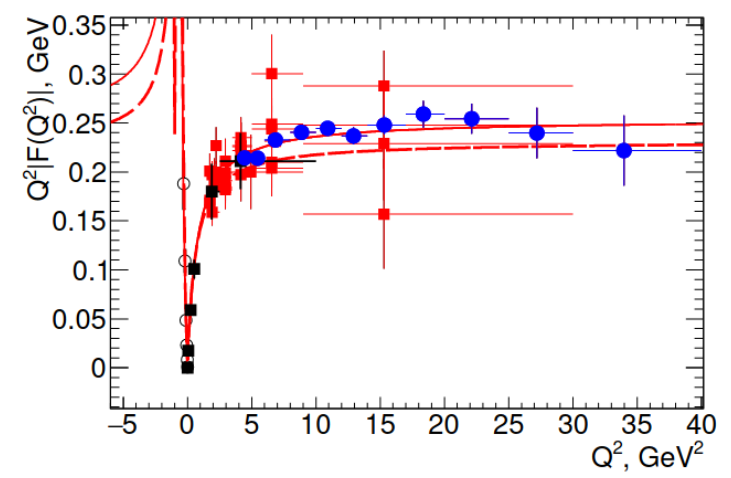
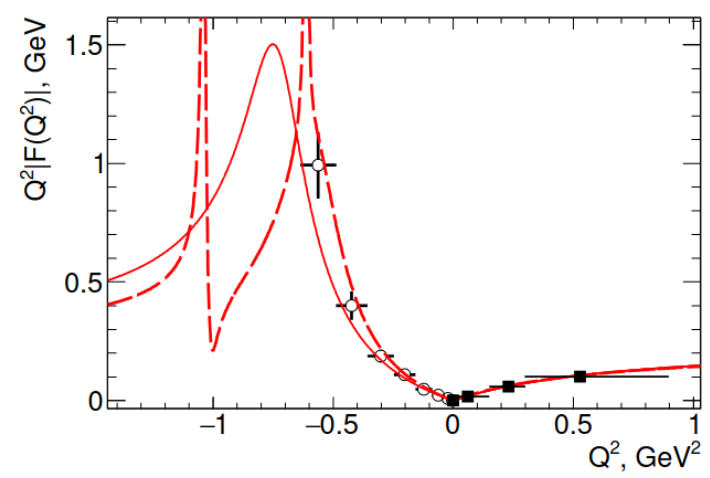
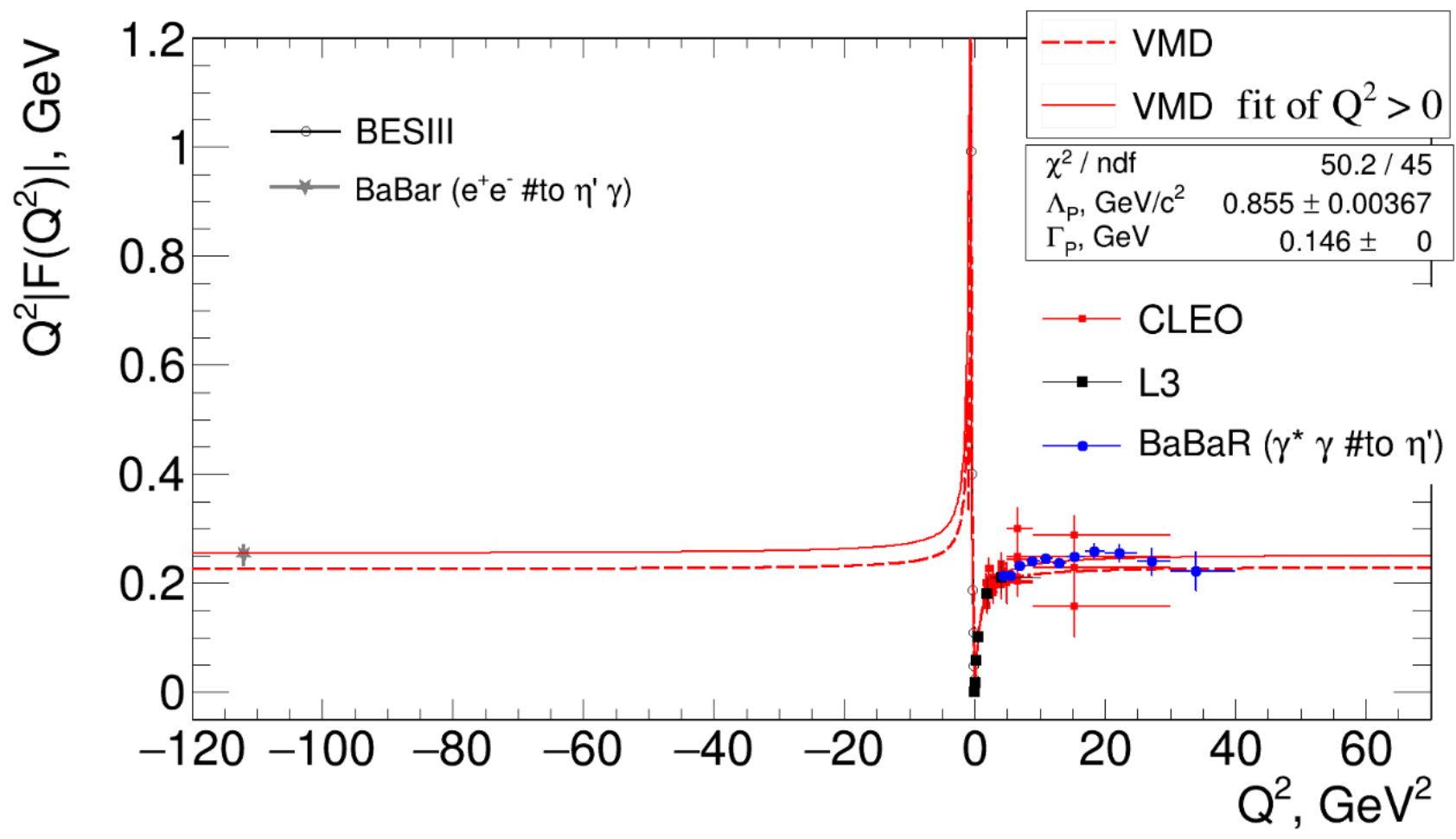
- The vector meson dominance model is commonly used to describe TFF at low Q^2 :



$$F_{\eta'}(Q_1^2, Q_2^2) = \frac{F_{\eta'}(0,0)}{(1 + Q_1^2/\Lambda_P^2)(1 + Q_2^2/\Lambda_P^2)}$$

- In case of the TFF with one off-shell photon the pQCD and VMD models leads to the same asymptotic behaviour $F(Q^2) \propto 1/Q^2$ at $Q^2 \rightarrow \infty$.

	VMD	pQCD
$Q_1^2 \approx 0, Q_2^2 \rightarrow \infty$	$1/Q^2$	$1/Q^2$
$Q_1^2, Q_2^2 \rightarrow \infty$	$1/Q^4$	$1/Q^2$



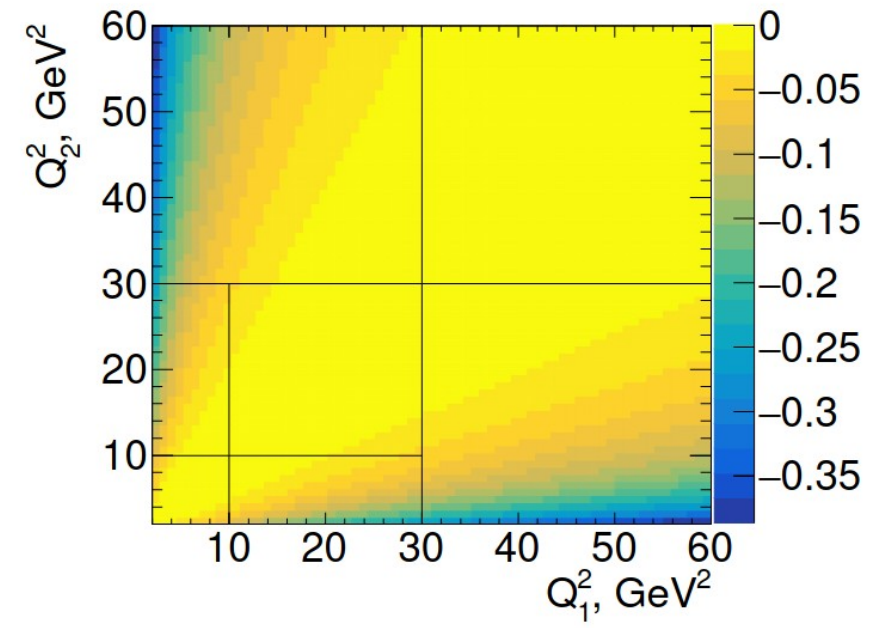
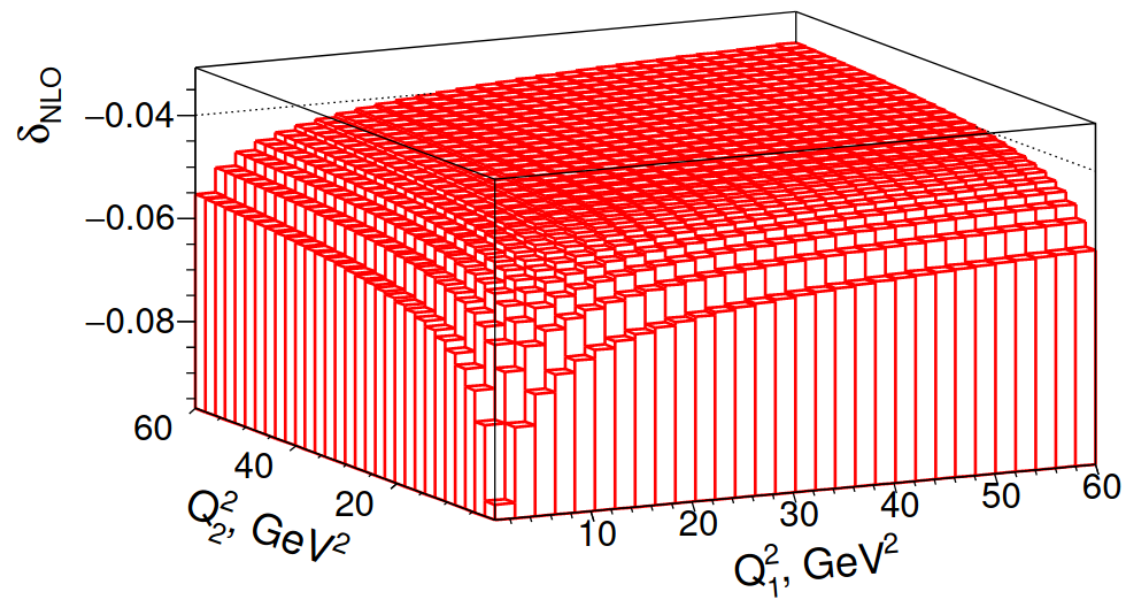
$$F_{\eta'}(Q_1^2, Q_2^2) = \left(\frac{5\sqrt{2}}{9} f_n \sin \phi + \frac{2}{9} f_s \cos \phi \right) \int_0^1 dx \frac{1}{2} \frac{6x(1-x)}{xQ_1^2 + (1-x)Q_2^2} \left(1 + C_F \frac{\alpha_s(\mu^2)}{2\pi} \cdot t(x, Q_1^2, Q_2^2) \right) + (x \rightarrow 1-x),$$

Master formula

The meson DA

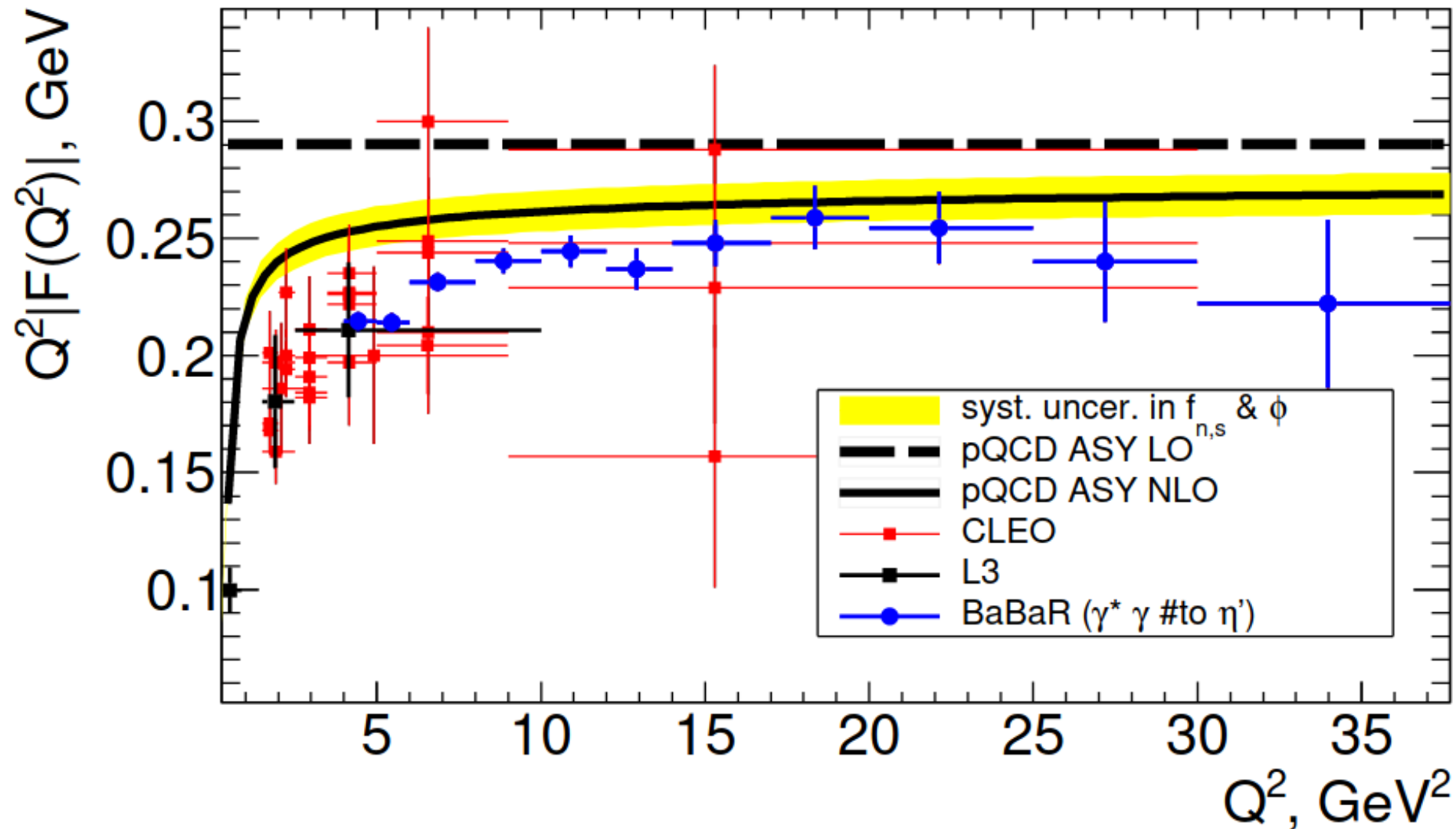
NLO

The form $1/(xQ_1^2 + (1-x)Q_2^2)$ is not divergent, so double-virtual transition FF is less sensitive to a shape of the meson DA than the single-virtual FF.



NLO contribution to the TFF

TFF dependence on DA

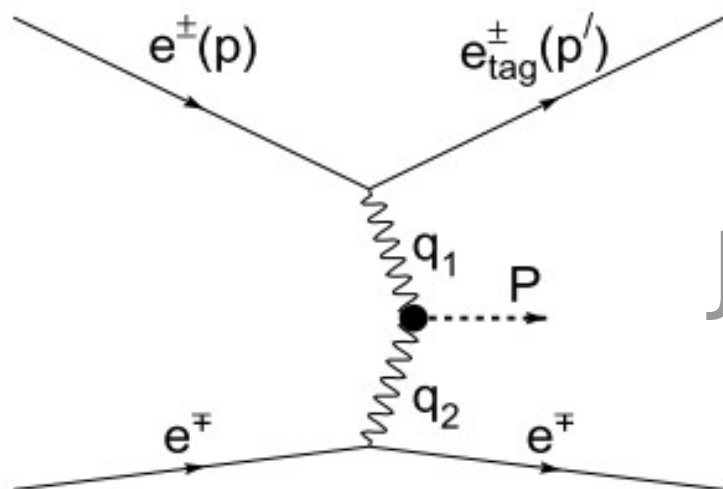


The $\gamma^ \gamma \rightarrow \eta'(958)$ Transition Form Factor*

The analysis is based on the previous BaBar study [1].

previous

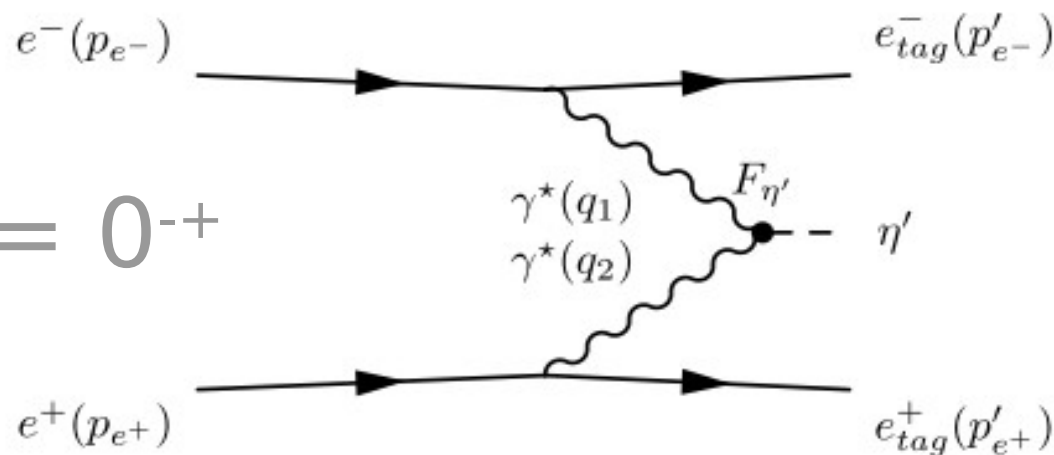
$\gamma\gamma^* \rightarrow \eta'$
 Single tagged
 ~ 5000 signal events



$$J^{PC} = 0^{-+}$$

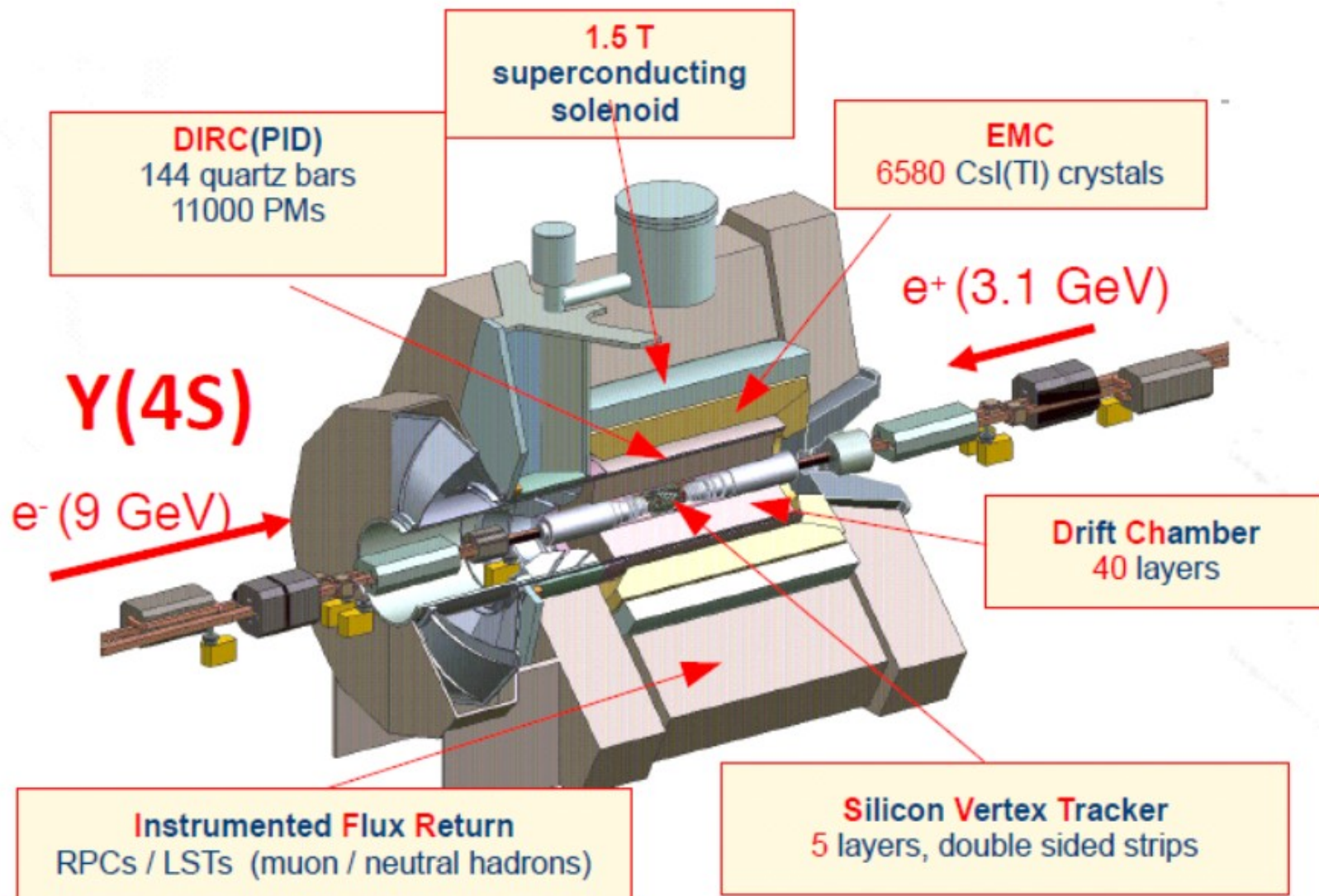
new

$\gamma^*\gamma^* \rightarrow \eta'$
 Double tagged
 46^{+8}_{-7} signal events



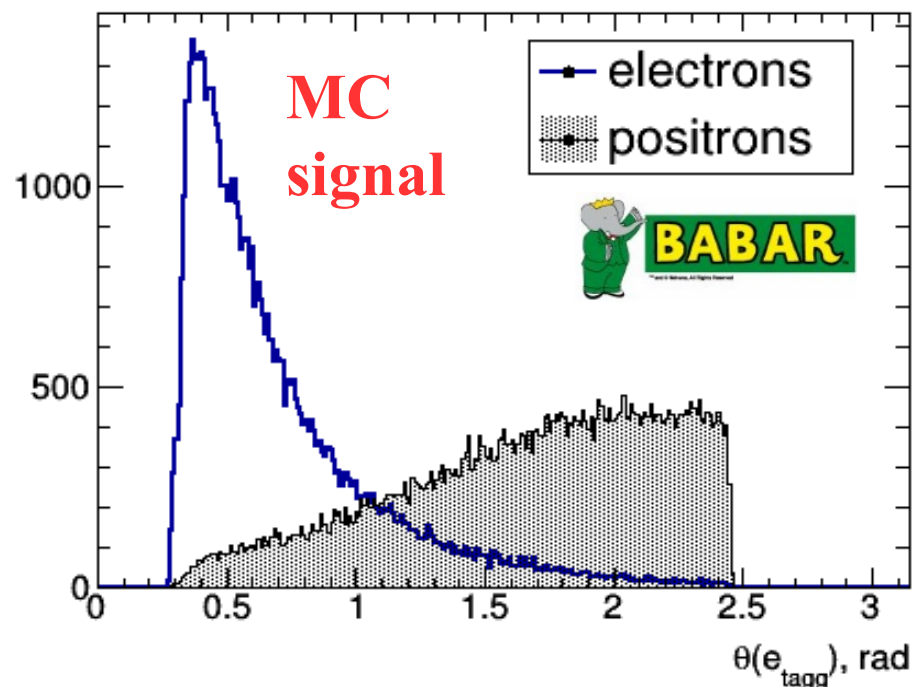
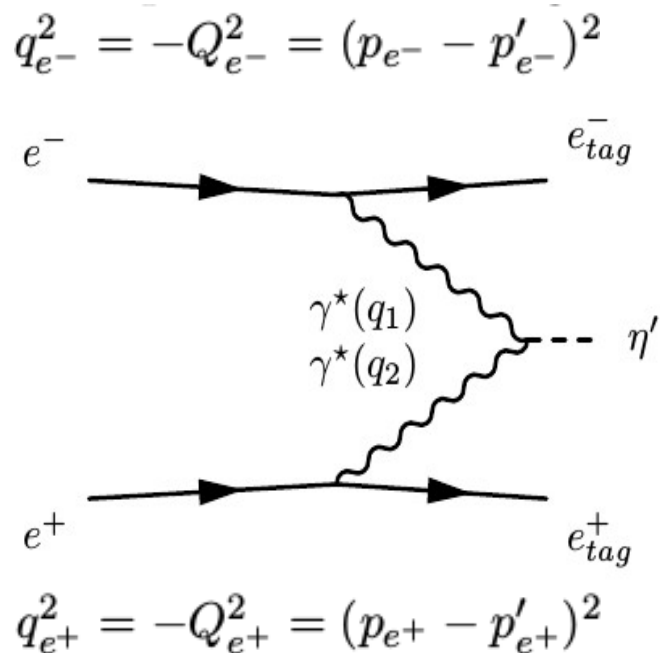
- A large number of systematic uncertainties were studied in our previous work where the number of signal events was significantly larger.

[1] [PRD 84, 052001]: **P. del Amo Sanchez et al. (BaBar collaboration), Phys. Rev. D 84, 052001 (2011) — (126 citations).**



BABAR detector at center-of mass energy of 10.6 GeV at the e^+e^- collider PEP-II at SLAC

Technique



- The decay chain $\eta' \rightarrow \pi^+ \pi^- \eta \rightarrow \pi^+ \pi^- 2\gamma$ is used *Polar angle distribution for tagged electrons (positrons)*
- A total integrated luminosity $L = 469 \text{ fb}^{-1}$
- GGResRc event generator is used [[arXiv:1010.5969](https://arxiv.org/abs/1010.5969)]. Initial and final state radiative corrections as well as vacuum polarization effects are included. The form factor is fixed to the constant value $F(0,0)$.

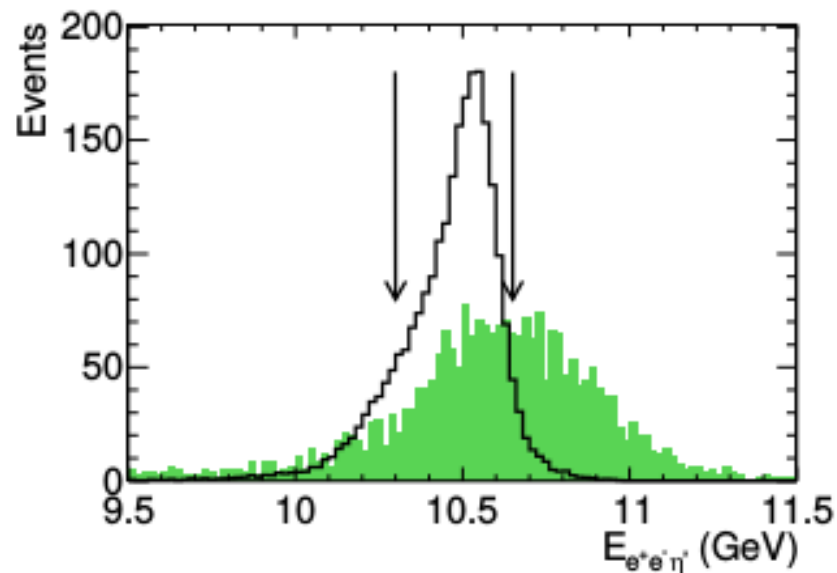
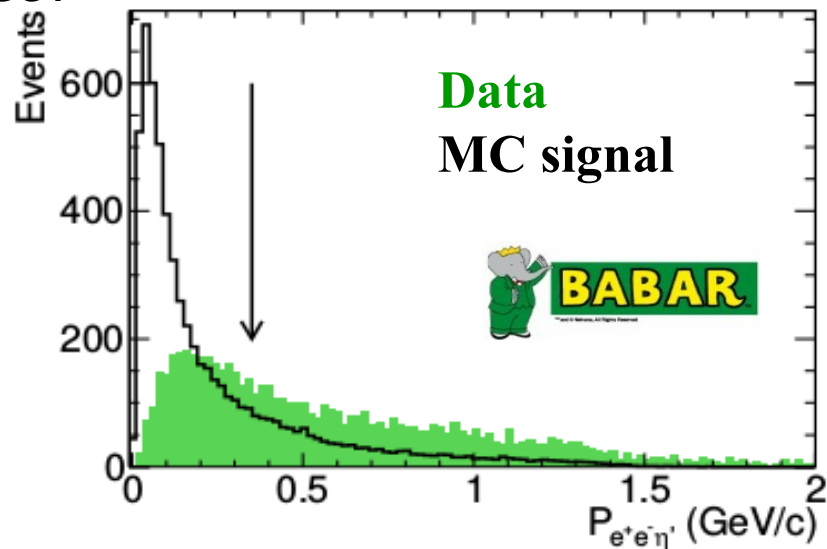
The strategy: $dN/dQ^2 \longrightarrow d\sigma/dQ^2 \longrightarrow |F(Q^2)|$

Event selection

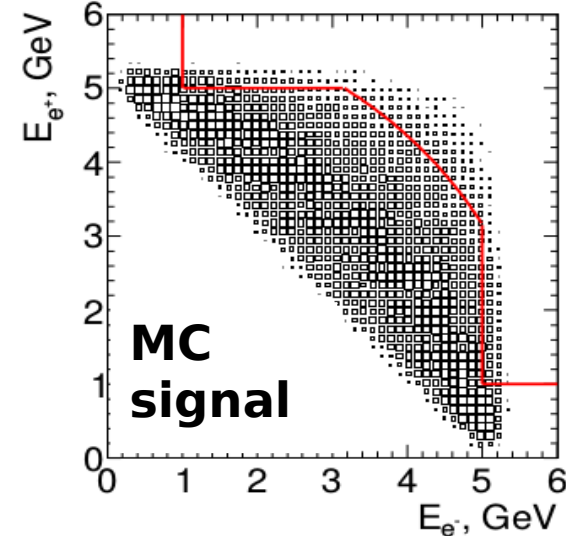
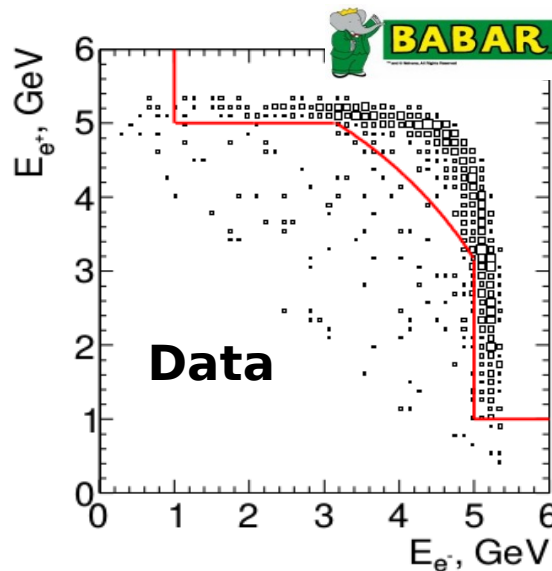
- The total reconstructed **momentum** of $e^+e^-\pi^+\pi^-\eta$ system in c.m. frame is less than 0.35 GeV/c.

- The total reconstructed **energy** of $e^+e^-\pi^+\pi^-\eta$ system in c.m. frame belongs to the range [10.3:10.7]

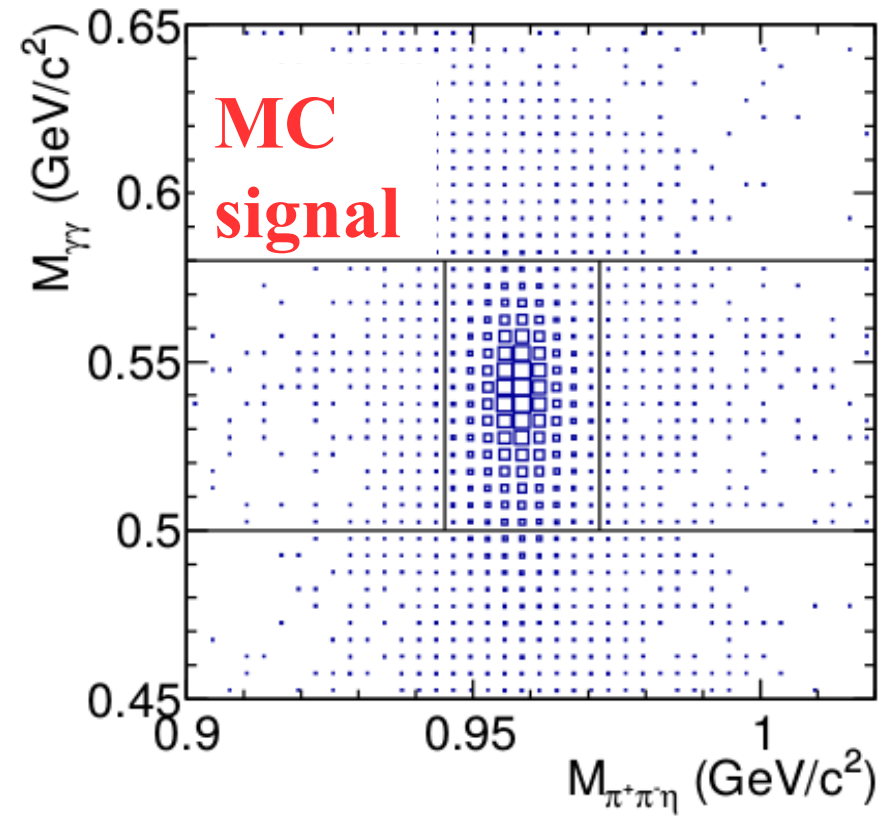
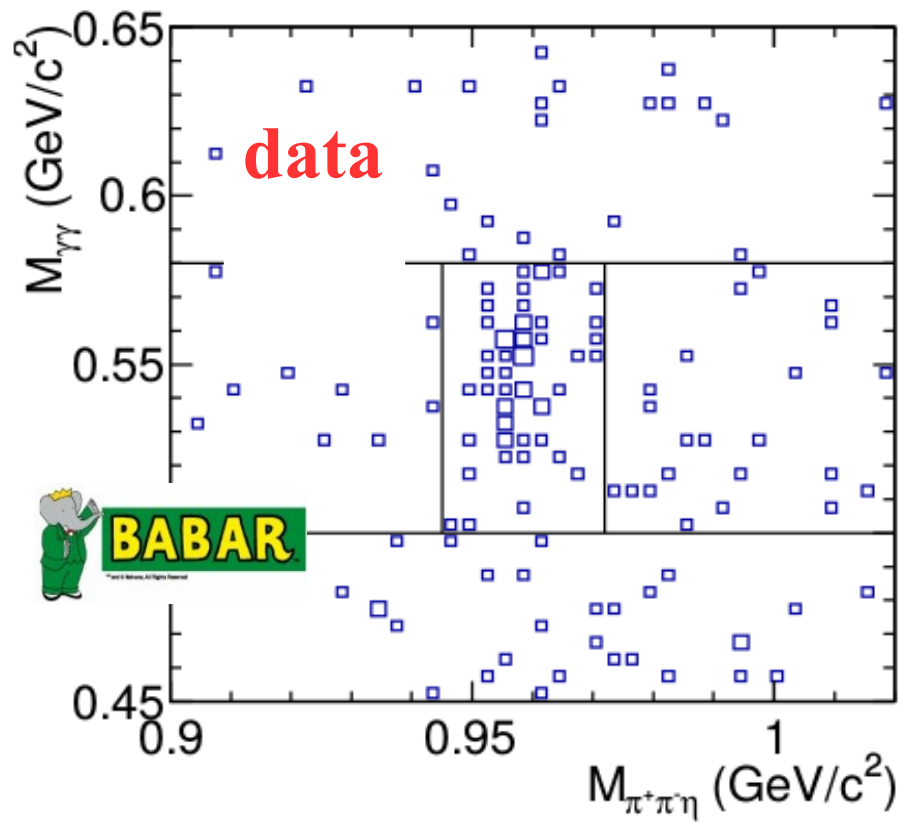
GeV



- Events that lie above and on the right of the lines (mostly, Bhabha scattering) are rejected.

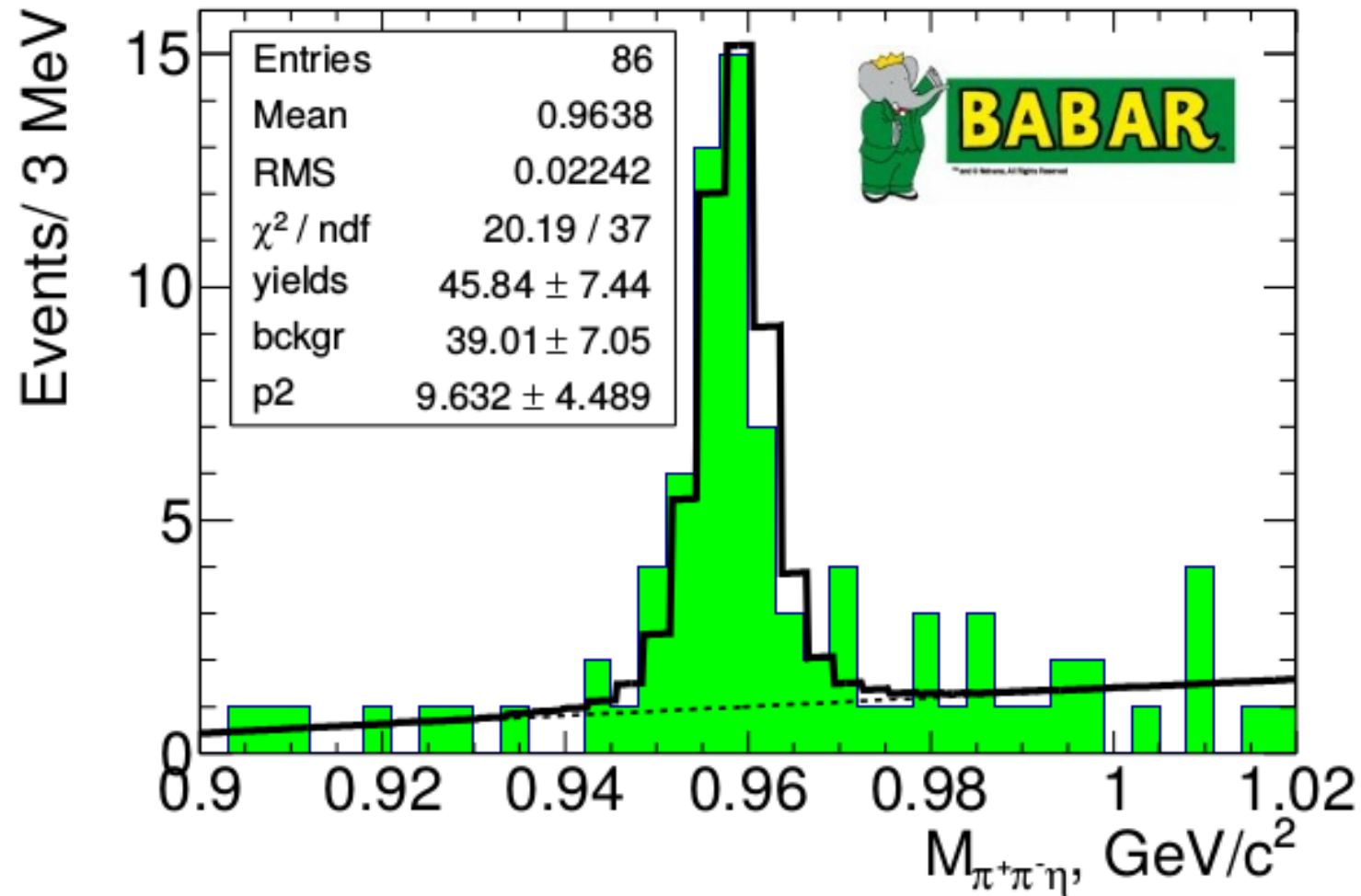


The positron c.m. energy vs. the electron c.m. energy

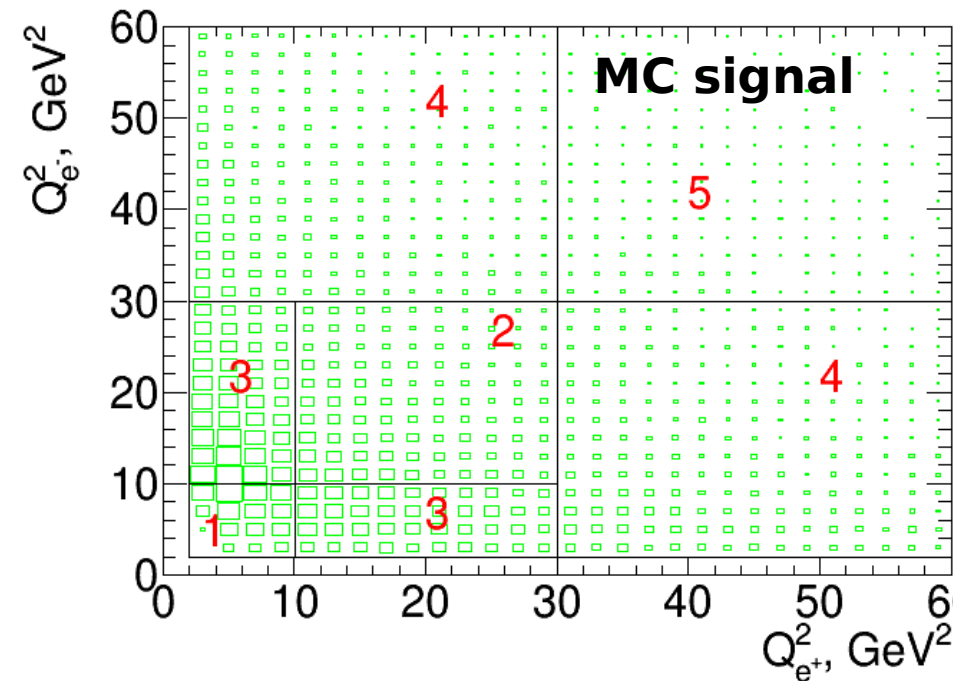
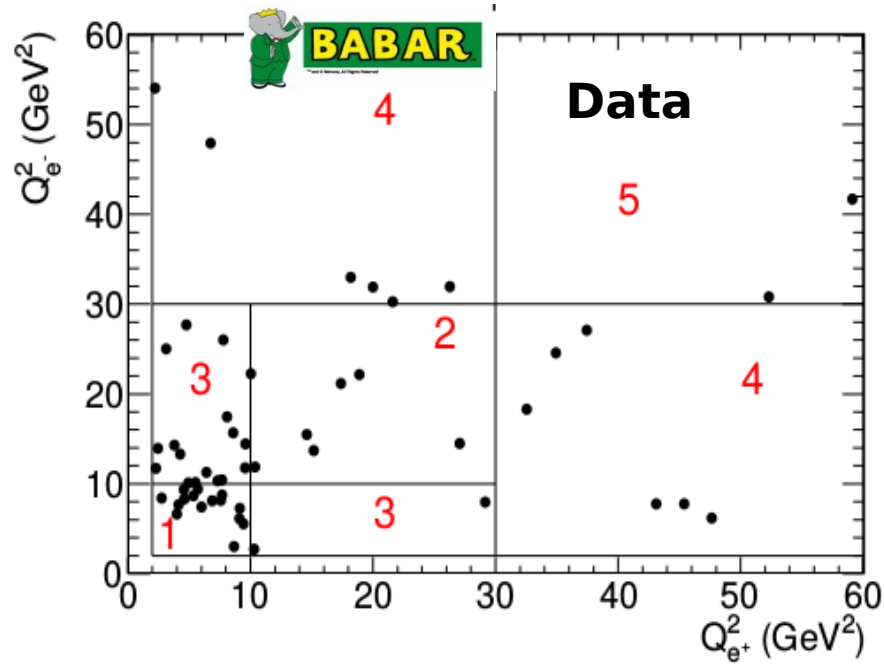


$m_{\gamma\gamma}$ vs. $m_{\pi^+\pi^-\eta}$

- We require $0.50 < m_{\gamma\gamma} < 0.58$ GeV/c²



The $\pi^+\pi^-\eta$ mass spectra for data events. The open histogram is the fit result. The dashed line represents fitted background.

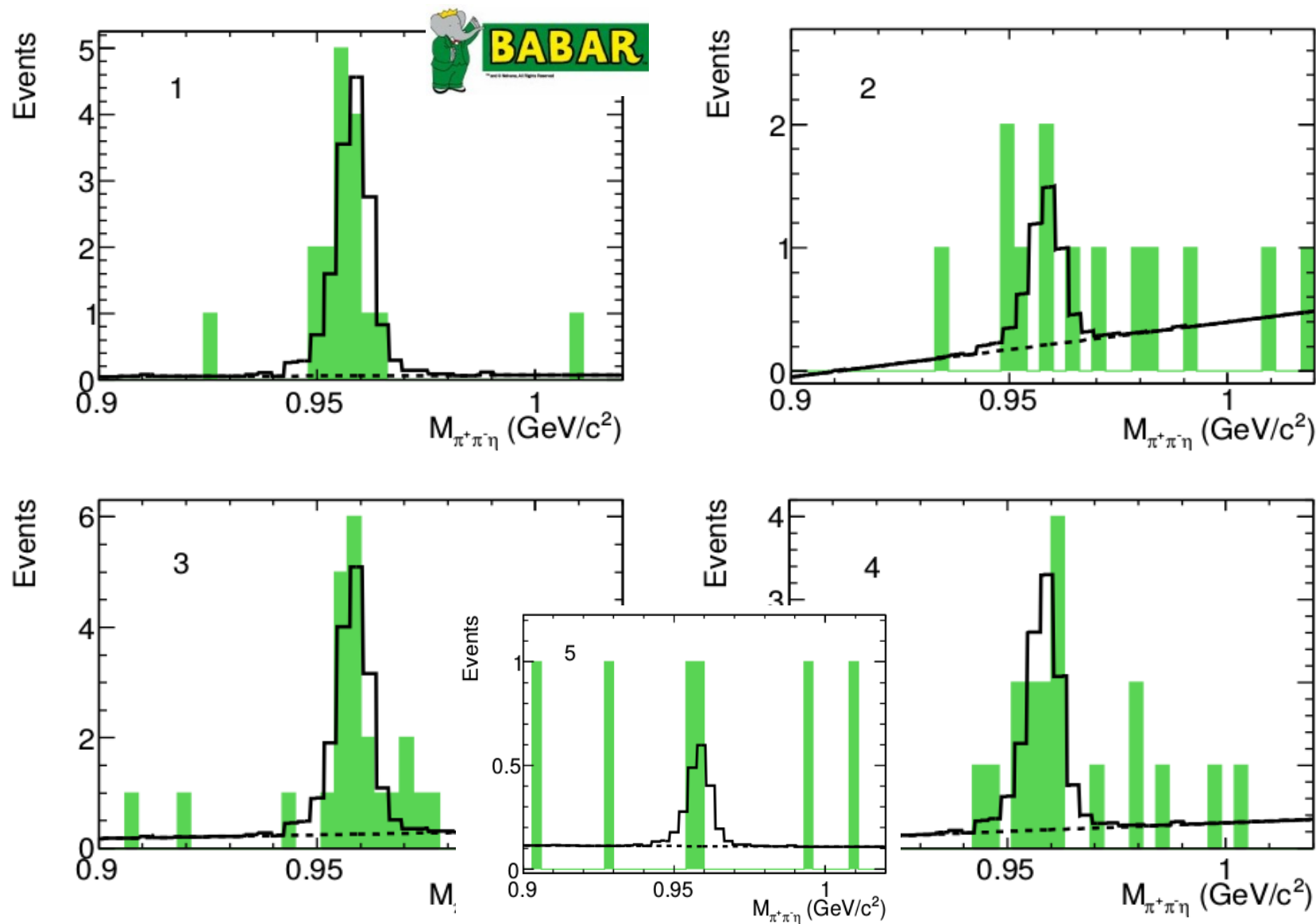


The $Q_{e^-}^2$ vs. $Q_{e^+}^2$ for events with $0.945 < m_{2\pi\eta} < 0.972$ GeV/c²

- New definition: $Q_1^2 = \max(Q_{e^+}^2, Q_{e^-}^2)$, $Q_2^2 = \min(Q_{e^+}^2, Q_{e^-}^2)$
- The average momentum transfers for each region are calculated using the data spectrum normalized to the detection efficiency:

$$\overline{Q_{1,2}^2} = \frac{\sum_i Q_{1,2}^2(i) / \varepsilon(Q_1^2, Q_2^2)}{\sum_i 1 / \varepsilon(Q_1^2, Q_2^2)}$$

- The total number of signal events $N^{\text{fit}}_{\text{signal}} = 46.2^{+8.3}_{-7.0}$



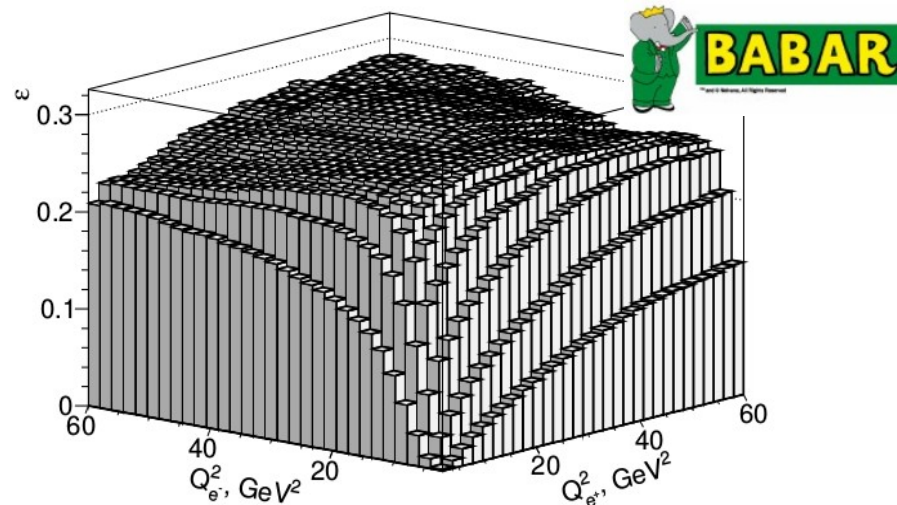
The $\pi^+\pi^-\eta$ mass spectra for data events for the five Q^2 ranges. The open histograms are the fit results. The dashed lines represent background.

Detection efficiency

- The detector acceptance limits the e^-e^+ detection efficiency at small Q^2 . The minimum Q^2 equals to 2 GeV^2 .

$$\epsilon_{true} = \frac{\int \epsilon(Q_1^2, Q_2^2) F_{\eta'}^2(Q_1^2, Q_2^2) dQ_1^2 dQ_2^2}{\int F_{\eta'}^2(Q_1^2, Q_2^2) dQ_1^2 dQ_2^2}$$

($F_{\eta'}$ from *master formula* at slide #7)



The dependence of detection efficiency on momentum transfers.

- Radiative corrections $R(Q_1^2, Q_2^2) = \frac{\sigma^{rad}(Q_1^2, Q_2^2)}{\sigma^{born}(Q_1^2, Q_2^2)}$
- R leads to the decrease of the detection efficiency by $\sim 15 \%$.
- The maximum energy of the photon emitted from the initial state is restricted by the requirement $E_\gamma < 0.05\sqrt{s}$, where \sqrt{s} is the e^+e^- center-of-mass (c.m.) energy.

- The differential cross section for $e^+e^- \rightarrow e^+e^-\eta'$ is calculated as

$$\frac{d^2\sigma}{dQ_1^2 dQ_2^2} = \frac{1}{\epsilon_{\text{true}} R L B} \frac{d^2 N}{dQ_1^2 dQ_2^2}$$

$$F^2(\overline{Q}_1^2, \overline{Q}_2^2) = \frac{(d^2\sigma/(dQ_1^2 dQ_2^2))_{\text{data}}}{(d^2\sigma/(dQ_1^2 dQ_2^2))_{\text{MC}}} F_{\eta'}^2(\overline{Q}_1^2, \overline{Q}_2^2)$$

- $B = B(\eta' \rightarrow \pi^+\pi^-\eta) \times B(\eta \rightarrow 2\gamma) = (0.3941 \pm 0.0020) \times (0.429 \pm 0.007) = 0.169 \pm 0.003$

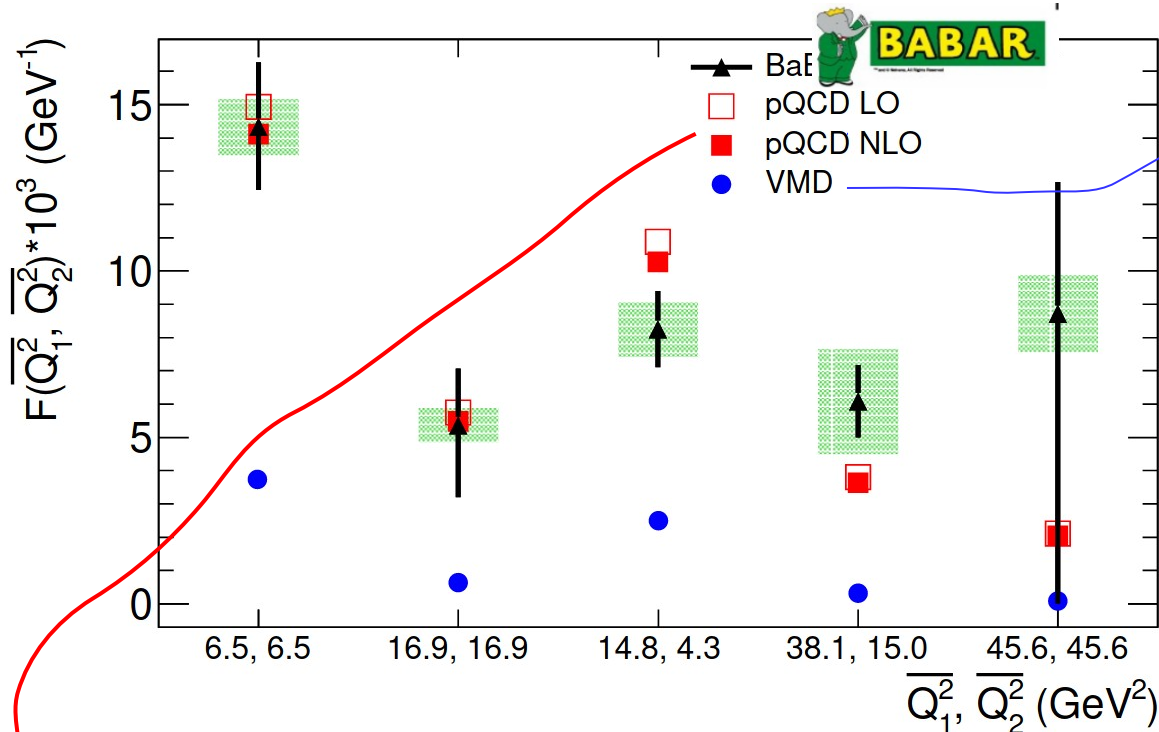
• $\sigma_{e^+e^- \rightarrow e^+e^-\eta'} (2 < Q_1^2, Q_2^2 < 60 \text{ GeV}^2) = (11.4^{+2.8}_{-2.4}) \text{ fb}$

$\overline{Q}_1^2, \overline{Q}_2^2, \text{ GeV}^2$	ϵ_{true}	R	N_{events}	$d^2\sigma/(dQ_1^2 dQ_2^2) \times 10^4, \text{ fb/GeV}^4$	$F(\overline{Q}_1^2, \overline{Q}_2^2) \times 10^3, \text{ GeV}^{-1}$
6.48, 6.48	0.019	1.03	$14.7^{+4.3}_{-3.6}$	$1471.8^{+430.1}_{-362.9}$	$14.32^{+1.95}_{-1.89} \pm 0.83 \pm 0.14$
16.85, 16.85	0.282	1.10	$4.1^{+2.7}_{-2.7}$	$4.2^{+2.8}_{-2.8}$	$5.35^{+1.54}_{-1.54} \pm 0.31 \pm 0.42$
14.83, 4.27	0.145	1.07	$15.8^{+4.8}_{-4.0}$	$39.7^{+12.0}_{-10.2}$	$8.24^{+1.16}_{-1.13} \pm 0.48 \pm 0.65$
38.11, 14.95	0.226	1.11	$10.0^{+3.9}_{-3.2}$	$3.0^{+1.2}_{-1.0}$	$6.07^{+1.09}_{-1.07} \pm 0.35 \pm 1.21$
45.63, 45.63	0.293	1.22	$1.6^{+1.8}_{-1.1}$	$0.6^{+0.7}_{-0.6}$	$8.71^{+3.96}_{-8.71} \pm 0.50 \pm 1.04$

Statistical
Systematic
Model

- Statistical uncertainty dominates

- $e^+e^- \rightarrow e^+e^- \eta' \pi^0 \rightarrow e^+e^- \pi^+ \pi^- \eta \pi^0$ - kinematically closest background for the process under study. Using the simulation of the $e^+e^- \rightarrow e^+e^- a_0(1450) \rightarrow e^+e^- \eta' \pi^0$ process we estimate the contribution $N_{\eta' \pi^0} < 0.16$ at 90% C.L.
- $e^+e^- \rightarrow e^+e^- J/\psi(\phi) \rightarrow e^+e^- \eta' \gamma$ as well as $e^+e^- \rightarrow \gamma^* \rightarrow X$ are also negligible.
- The systematic uncertainty (12%) of cross section is dominated by the uncertainty related to selection criteria (11%).
- Predominantly, the model uncertainty arises from the model dependence of $(d^2\sigma/(dQ^2_1 dQ^2_2))_{MC}$ and ϵ_{true} .
Repeating the calculations with a constant TFF we estimate the model uncertainty.
For the cross section - about 60% due to the strong dependence of ϵ_{true} on the input model for TFF at small values of Q^2_1 and Q^2_2 .
However, the TFF is much less sensitive to the model.



$$F_{\eta'}(Q_1^2, Q_2^2) = \frac{F_{\eta'}(0, 0)}{(1 + Q_1^2/\Lambda_P^2)(1 + Q_2^2/\Lambda_P^2)}$$

The Λ_P is fixed at 849 MeV/c² from the approximation of $F_{\eta'}(Q^2, 0)$ with one off-shell photon [Phys. Rev. D 85, 057501 (2012)].

The comparison of obtained form-factor with theoretical predictions

$$F_{\eta'}(Q_1^2, Q_2^2) = \left(\frac{5\sqrt{2}}{9} f_n \sin \phi + \frac{2}{9} f_s \cos \phi \right) \int_0^1 dx \frac{1}{2} \frac{6x(1-x)}{xQ_1^2 + (1-x)Q_2^2} \left(1 + C_F \frac{\alpha_s(\mu^2)}{2\pi} \cdot t(x, Q_1^2, Q_2^2) \right) + (x \rightarrow 1-x),$$

NLO

- pQCD calculation is in good agreement with data ($\chi^2/\text{n.d.f.} = 6.2/5$, Prob = 28%)
- VMD model exhibits a clear disagreement with the experiment

On some implications of the BaBar data on the $\gamma^*\eta'$ transition form factor

Peter Kroll (Wuppertal U.), Kornelija Passek-Kumerički (Boskovic Inst., Zagreb)

Mar 15, 2019

5 pages

Published in: *Phys.Lett.B* 793 (2019) 195-199

e-Print: [1903.06650](https://arxiv.org/abs/1903.06650) [hep-ph]

\bar{Q}^2 [GeV ²]	ω	$\bar{Q}^2 F_{\eta'\gamma^*}^{\text{exp}}$ [MeV]	$\bar{Q}^2 F_{\eta'\gamma^*}$ [MeV]	χ^2	$\bar{Q}^2 F_{\eta\gamma^*}$ [MeV]
6.48	0.000	92.8 ± 13.8	92.7 ± 3.9	0.00	56.2 ± 3.3
16.85	0.000	90.1 ± 37.3	93.8 ± 3.9	0.01	56.8 ± 3.3
9.55	0.553	78.7 ± 13.5	98.7 ± 4.1	2.19	59.9 ± 3.5
26.53	0.436	161.0 ± 44.2	97.7 ± 4.1	2.05	59.2 ± 3.5
45.63	0.000	397.4 ± 400.9	94.6 ± 4.0	0.57	57.4 ± 3.4

Predictions of transition form factors with
NLO meson distribution amplitude

The improvement of accuracy in the further experiments will allow:

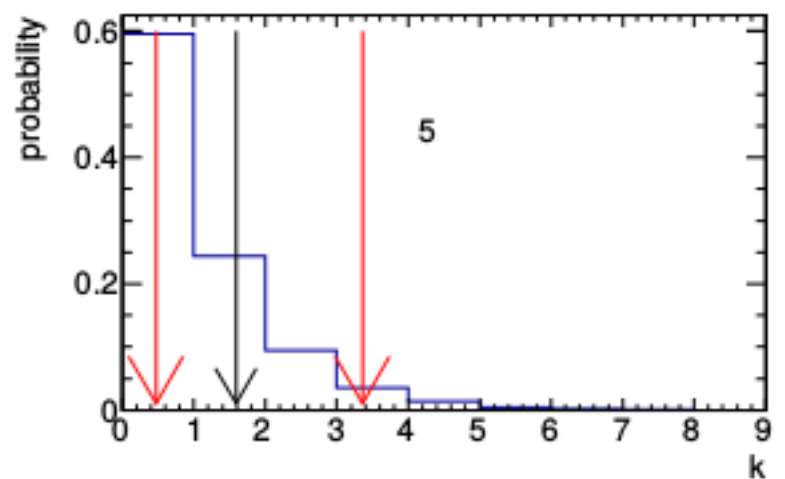
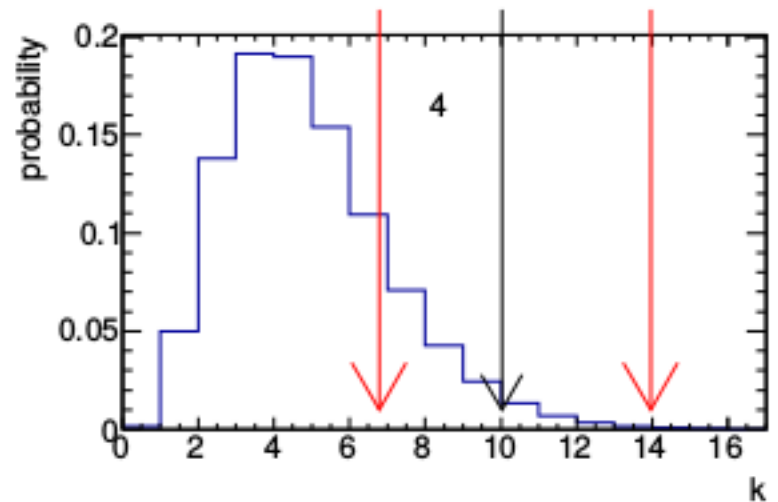
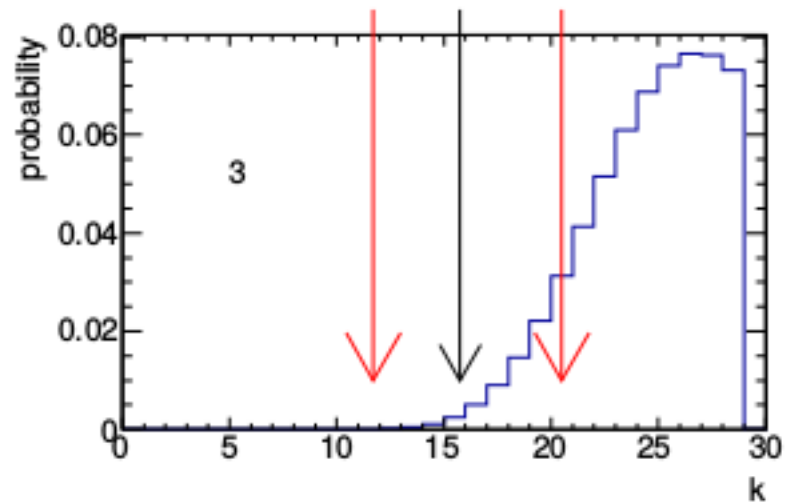
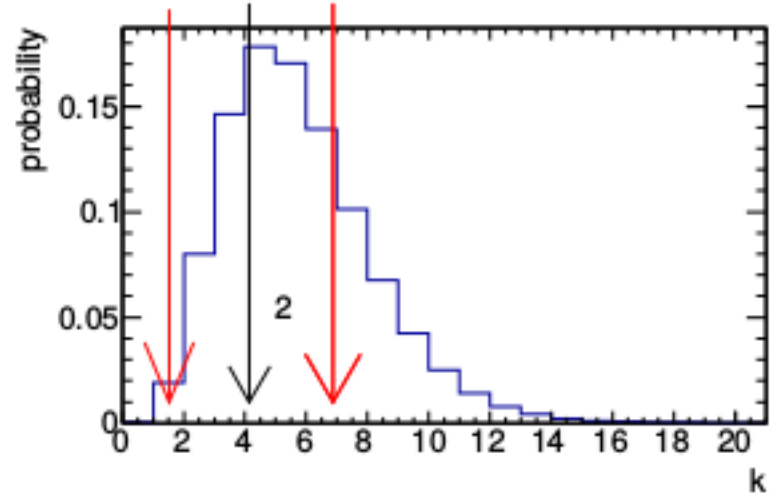
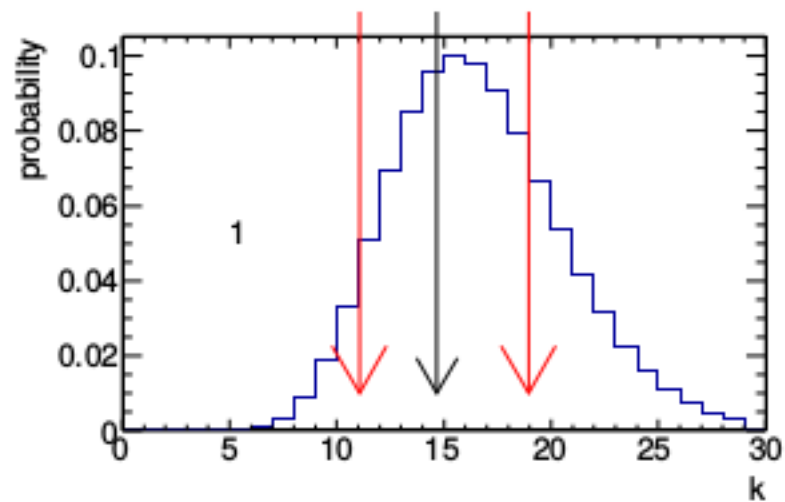
1. measuring of quarks distribution amplitudes
2. measuring of contribution from NLO twist



- About 46 events of $e^+e^- \rightarrow e^+e^-\eta'(958)$ were observed in the double tagged mode for the first time.
- The $\gamma^*\gamma^* \rightarrow \eta'(958)$ transition form factor $F(Q_1^2, Q_2^2)$ have been measured for Q^2 range from 2 to 60 GeV^2 .
- The form factor is in reasonable agreement with the pQCD prediction.

Thank you!

Back up slides



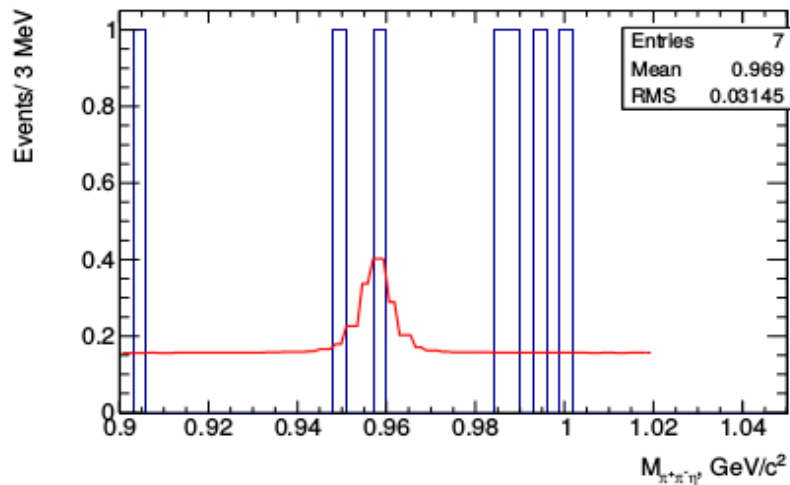
k — Poisson probability for k number of events to be detected according to pQCD;

Black arrow — the number of observed signal events;

Red arrows — the window of errors from fit.

Background subtraction

- $e^+e^- \rightarrow e^+e^-\eta'\pi^0 \rightarrow e^+e^-\pi^+\pi^-\eta\pi^0$ - kinematically closest background for the process under study.
- We perform the search of the process using all BaBar data and the same technique as for $e^+e^- \rightarrow e^+e^-\eta'$ with additional requirements for π^0 .
- We simulate the process via the mechanism $e^+e^- \rightarrow e^+e^-a_0(1450) \rightarrow e^+e^-\eta'\pi^0$. More details can be found in BAD#2689.



$$N_{\eta'\pi^0}^{signal} < 1.45 \text{ at } 90\% \text{ C.L.}$$

The $\pi^+\pi^-\eta$ invariant mass spectrum

The detection efficiency for $e^+e^-\eta'\pi^0$ events to pass the selections of $e^+e^-\eta'$.

$$N_{bkg} = \frac{N_{\eta'\pi^0}^{signal} \epsilon_{\eta'\pi^0}^{(2)}}{\epsilon_{\eta'\pi^0}^{(1)}} < 0.16 \text{ at } 90\% \text{ C.L.}$$

The detection efficiency for $e^+e^-\eta'\pi^0$ events to pass the selections of $e^+e^-\eta'\pi^0$.

The main source of systematic uncertainty of cross section

Source	Uncertainty (%)
π^\pm identification	1.0
e^\pm identification	1.0
Other selection criteria	11
Track reconstruction	0.9
$\eta \rightarrow 2\gamma$ reconstruction	2
Trigger, filters	1.3
Background subtraction	3.7
Radiative correction	1.0
Luminosity	1.0
Total	12%

from previous BaBar study of $\gamma^*\gamma \rightarrow \eta'$
 Phys. Rev. D 74 012002 (2006)

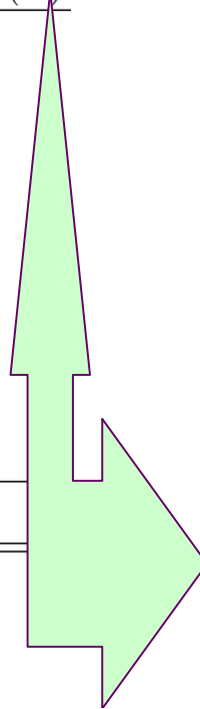
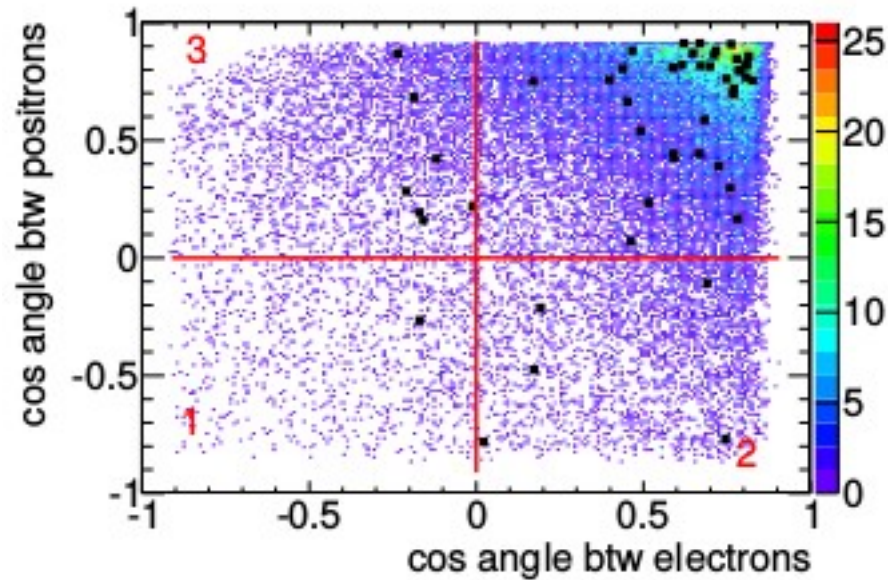


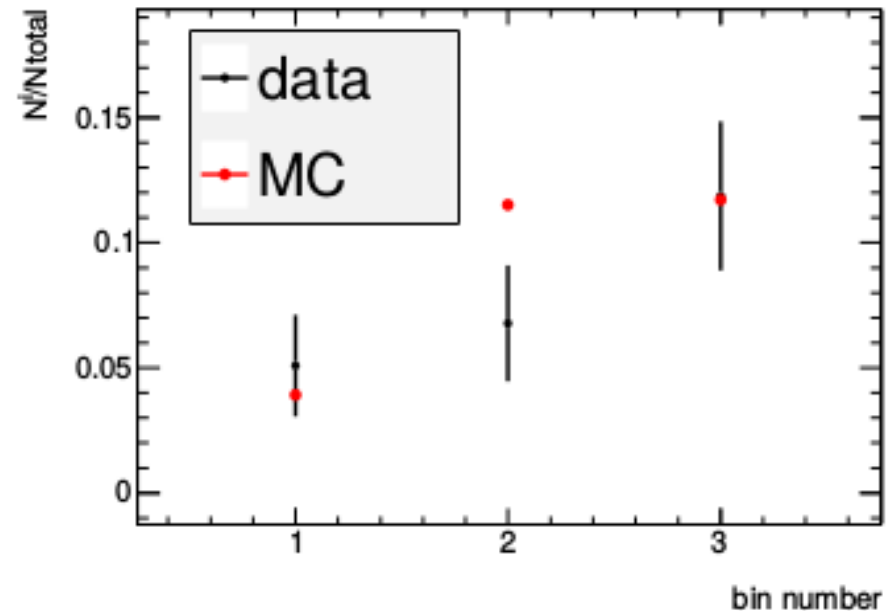
TABLE IV: The result of the study of the uncertainty associated with the selection criteria

selection	$N_{signal}/\epsilon_{true}$	deviation from standard criteria
standard selection criteria	985 ± 197	
$P_{e^+e^-\eta'}$ is less than 1 GeV/c instead of 0.35 GeV/c	1052 ± 273	6.8
$10.20 < E_{e^+e^-\eta'} < 10.75$ GeV instead of $10.3 < E_{e^+e^-\eta'} < 10.65$ GeV	942 ± 235	-4.3
without the restrictions on E_{e^+} and E_{e^-}	1061 ± 280	7.7
$0.48 < m_{2\gamma} < 0.60$ GeV/c ² instead of $0.50 < m_{2\gamma} < 0.58$ GeV/c ²	958 ± 181	-2.7
total		11

- $e^+e^- \rightarrow e^+e^- J/\psi(\phi) \rightarrow e^+e^- \eta' \gamma$ is negligible according to [PRD 84, 052001].
- $e^+e^- \rightarrow \gamma^* \rightarrow X$

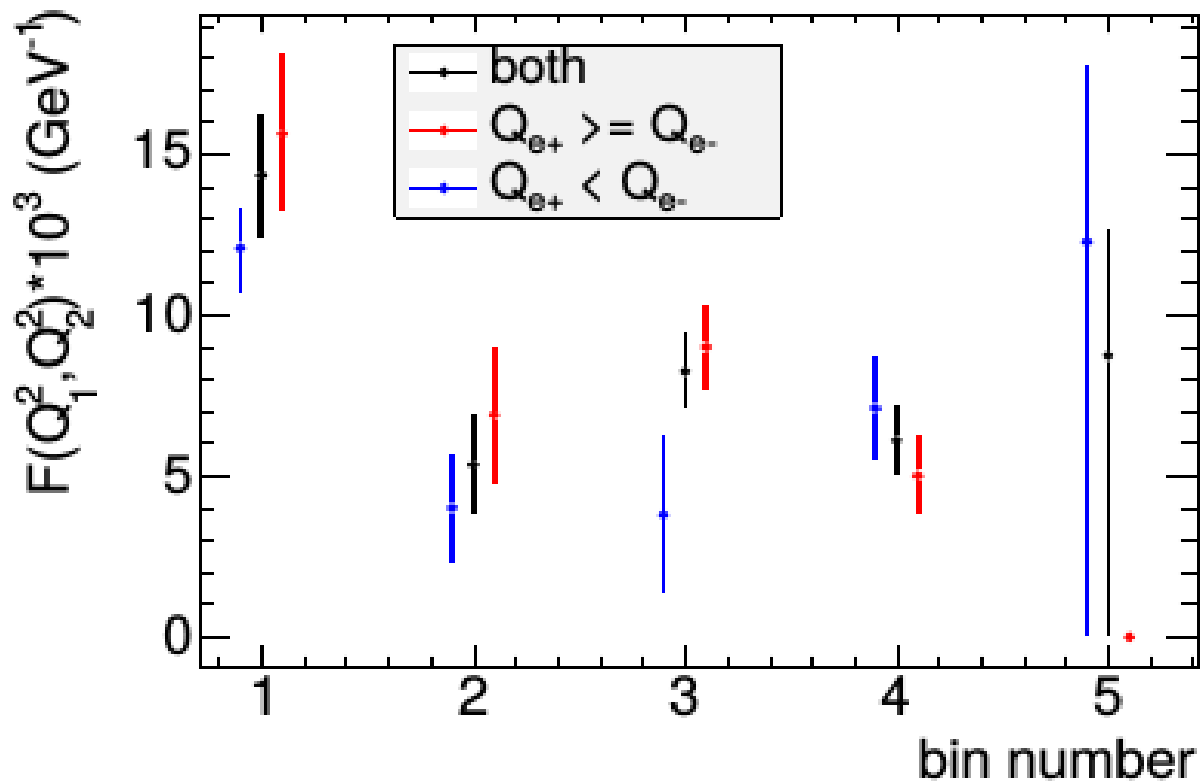


The cosine of angle between scattered and initial electron (positron) in c.m.f.



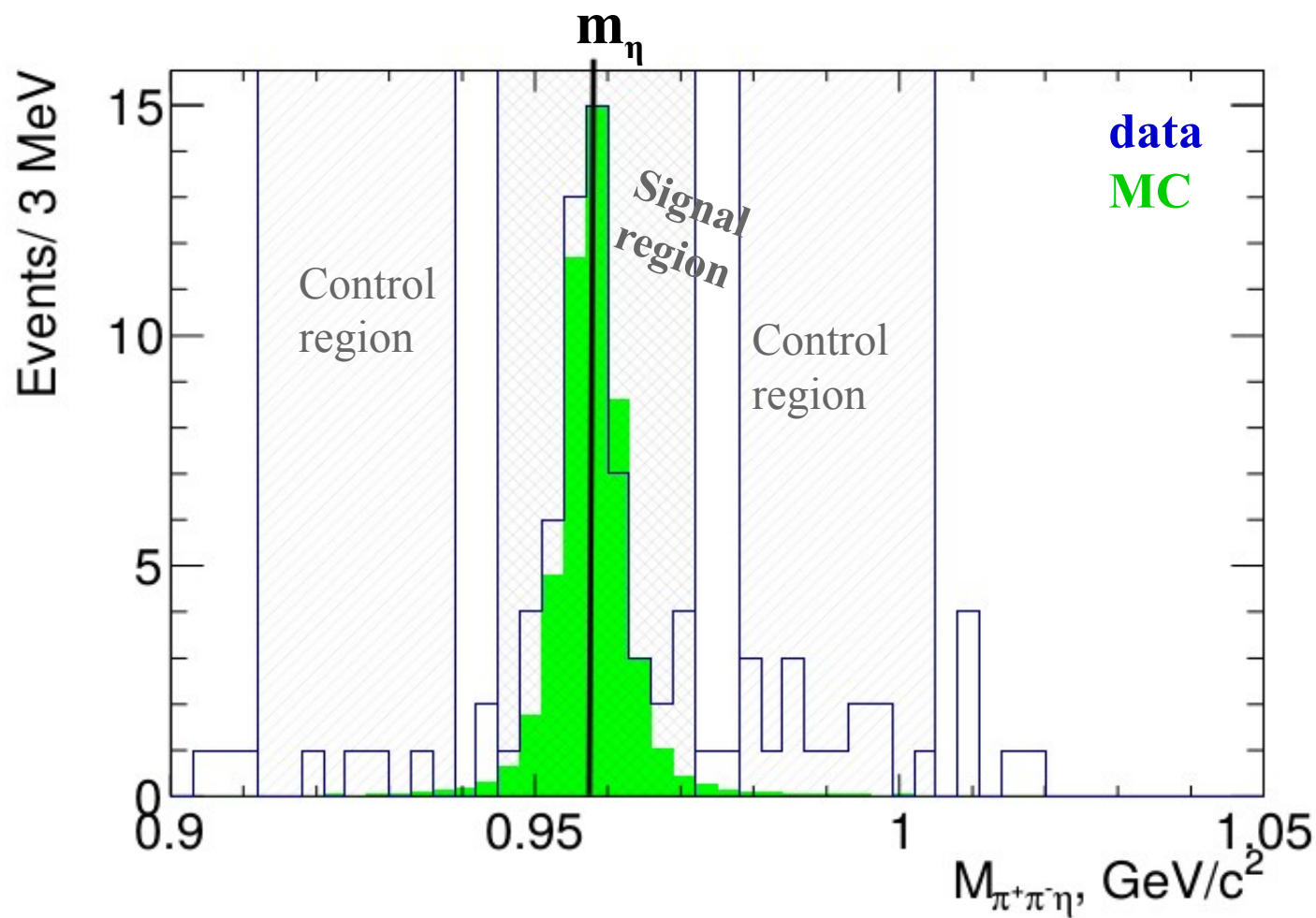
The fraction of the events in the bins.

It is reasonable to assume that the $\cos(\alpha_{e^\pm})$ spectrums must be symmetric in $[-1:1]$ region for **annihilation processes**, while signal scattered electron (positron) prefers to fly in the about the same direction.



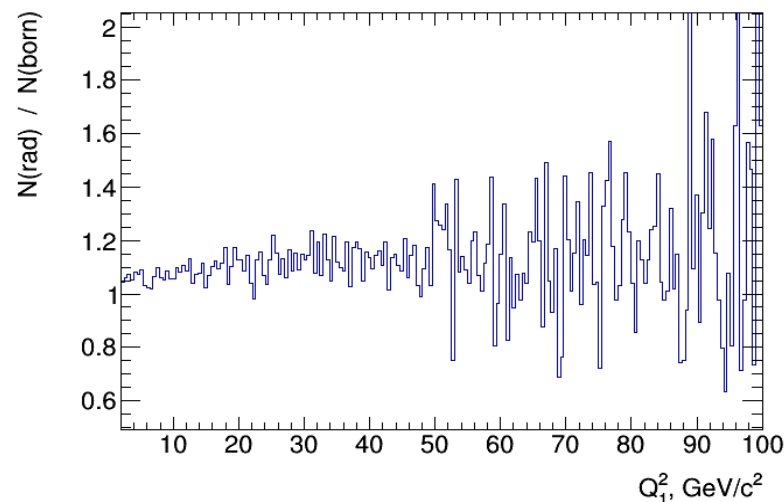
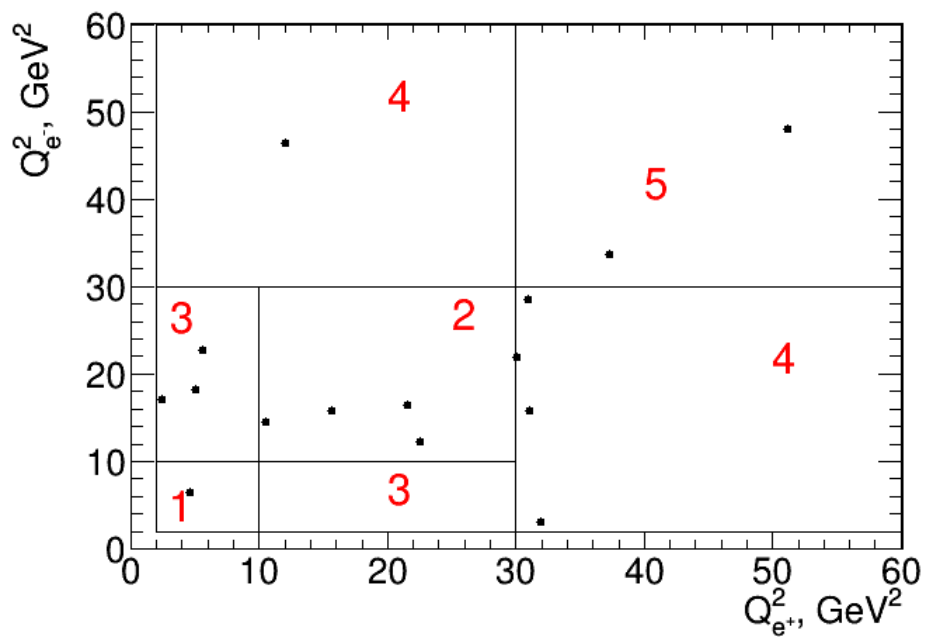
The comparison of the measured η' TFF with $Q_{e+}^2 < Q_{e-}^2$, $Q_{e+}^2 \geq Q_{e-}^2$ and without the restriction.

Event selection

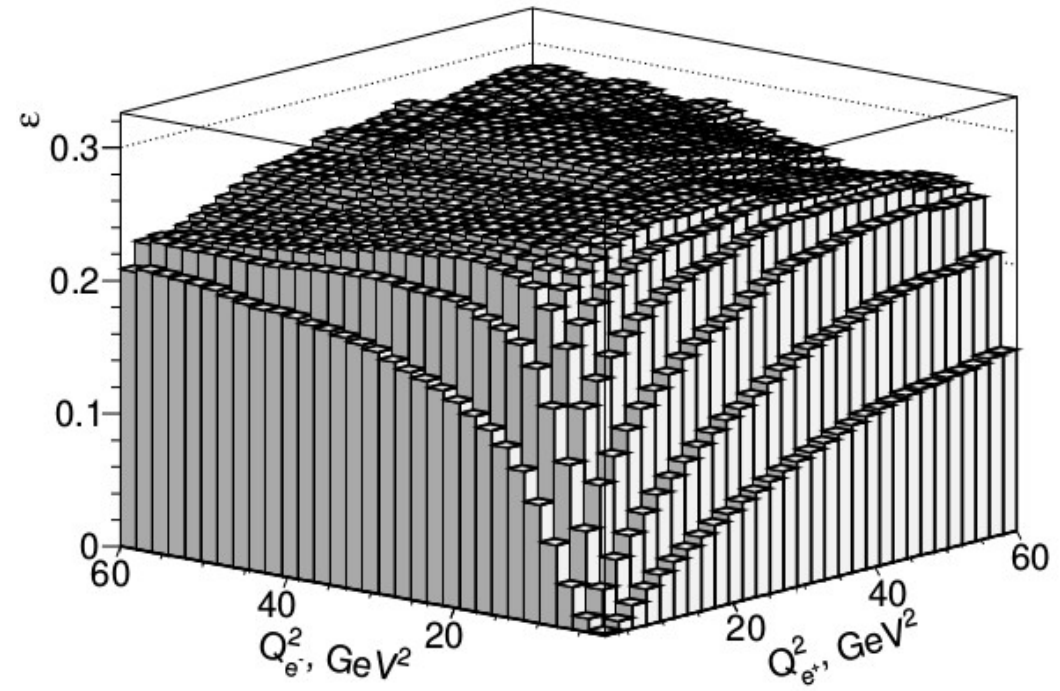


The data-MC comparison of $\pi\pi\eta$ invariant mass distribution. The MC histogram is normalized to central bin of data distribution.

The expected number of signal $N_{\text{signal}}^{\text{side}} = 55 - 18/2 = 46$



The ratio of generated spectra with rad. photons vs. without photons



The dependence of detection efficiency on momentum transfers.

We require the presense

- at least **two tracks** from *GoodTrackLoose* list passed *LooseElectronMicroSecection*
 - $-0.3 < \theta_e < 2.45$ radians
- at least **two tracks** from *GoodTrackLoose* list passed *TightKMPionMicroSelection*
 - $-0.45 < \theta_\pi < 2.4$ radians
- at least **two photons** from *GoodPhotonLoose* list
 - $\epsilon_\gamma > 30$ MeV
 - $-0.45 < m_{\gamma\gamma} < 0.65$ GeV/c²
 - The photon candidates are fitted with a η mass constraint.
- The η candidate and a pair of oppositely-charged pion candidates are fitted with a η' mass constraint.

TABLE V: $\frac{d^2\sigma}{dQ_1^2 dQ_2^2}$ obtained with different models for TFF

	1	2	3	4	5
QCD	$1471.8^{+430.136}_{-362.91}$	$4.17^{+2.75}_{2.75}$	$39.72^{+11.98}_{-10.18}$	$2.98^{+1.17}_{-0.96}$	$0.62^{+0.69}_{-0.62}$
const	$637.10^{+186.19}_{-157.09}$	$4.15^{+2.74}_{2.74}$	$33.30^{+10.05}_{-8.54}$	$2.76^{+1.08}_{-0.89}$	$0.62^{+0.69}_{-0.62}$
deviation, %	60	0.6	15	7	1.

TABLE VI: TFF obtained with different models for TFF

	1	2	3	4	5
QCD	$14.32^{+1.95}_{-1.89}$	$5.35^{+1.54}_{-1.54}$	$8.24^{+1.16}_{-1.13}$	$6.07^{+1.09}_{-1.07}$	$8.71^{+3.96}_{-8.71}$
const	$14.61^{+1.99}_{-1.92}$	$5.62^{+1.62}_{-1.62}$	$7.24^{+1.02}_{-0.99}$	$7.24^{+1.30}_{-1.28}$	$10.02^{+4.55}_{-10.02}$
deviation %	1	8	8	20	12